

Influence of a parallel magnetic field on the microwave photoconductivity in a high-mobility two-dimensional electron system

C. L. Yang,^{1,2} R. R. Du,^{1,2} L. N. Pfeiffer,³ and K. W. West³¹*Department of Physics and Astronomy, Rice University, Houston, Texas 77005, USA*²*Department of Physics, University of Utah, Salt Lake City, Utah 84112, USA*³*Bell Laboratories, Lucent Technologies, Murray Hill, New Jersey 07974, USA*

(Received 27 March 2006; published 18 July 2006)

Using a two-axis magnet, we have studied experimentally the influence of a parallel magnetic field (B_{\parallel}) on microwave-induced resistance oscillations (MIROs) and zero-resistance states (ZRS) previously discovered in a high-mobility two-dimensional electron system. We have observed a strong suppression of MIRO/ZRS by a modest $B_{\parallel} \sim 1$ T. In Hall bar samples, magnetoplasmon resonance (MPR) has also been observed concurrently with the MIRO/ZRS. In contrast to the suppression of MIRO/ZRS, the MPR peak is apparently enhanced by B_{\parallel} . These findings cannot be explained by a simple modification of single-particle energy spectrum and/or scattering parameters by B_{\parallel} .

DOI: 10.1103/PhysRevB.74.045315

PACS number(s): 73.40.-c, 73.43.-f, 73.21.-b

Microwave- (MW-) induced resistance oscillations¹ (MIROs) and zero-resistance states (ZRS),²⁻⁶ observed in a high-mobility two-dimensional electron system (2DES) in GaAs/AlGaAs heterostructures, have been the subject of intense current interest in the condensed matter community.⁷ It has been theoretically shown⁸ that the ZRS is the direct consequence of an instability caused by absolute negative conductivity (ANC), occurring at the oscillation minima when the MIRO are sufficiently strong. The instability leads to the formation of electric current domains with zero voltage, resulting in a measured zero resistance. In this context, a large number of microscopic mechanisms have been proposed to account for the MIRO and the subsequent ANC, based on MW-assisted electron scattering⁹ or MW-induced nonequilibrium electron distribution^{4,10} and the oscillatory density of states due to Landau quantization. Other interesting mechanisms, such as those focusing on the orbit dynamics^{11,12} or quantum interference effect,¹³ have been proposed.

Recently, the importance of electrodynamic effects has been reemphasized¹⁴⁻¹⁶ for the microwave response of a high-mobility 2DES. Specifically, the plasmon modes are expected to play a role on the MIRO and ZRS in real samples with finite size. It is well known that, for a 2DES with lateral width w , the (bulk) magnetoplasmon resonance (MPR) occurs at^{17,18}

$$\omega = \sqrt{\omega_c^2 + \omega_0^2}, \quad (1)$$

where the MW frequency $\omega = 2\pi f$, the cyclotron frequency $\omega_c = eB/m^*$, and the 2D-plasmon frequency $\omega_0 = \sqrt{n_e e^2 q / 2\epsilon\epsilon_0 m^*}$, with an effective dielectric constant $\epsilon = (1 + \epsilon_{\text{GaAs}})/2 = 6.9$ for GaAs, and a plasmon wave vector $q = \pi/w$. The MPR has been previously observed, together with MIRO, in MW photoconductivity of a lower-mobility 2DES.¹ However, so far it has not been reported in ultraclean samples where ZRS are observed. The role of MPR is an unsettled issue relevant to the origin of the MIRO and ZRS.¹⁴

In this paper, we report on the influence of a parallel magnetic field on the MW photoconductivity of ultraclean

2DES. The MIRO and ZRS, as well as the MPR, are experimentally studied under a fixed parallel magnetic field (B_{\parallel}) and sweeping perpendicular field (B_z), with B_z and B_{\parallel} being independently provided by a two-axis magnet. Our main finding is that the oscillatory photoconductivity is *strongly* suppressed by a relatively small B_{\parallel} , of the order of 1 T. And we found that the MPR can occur *concurrently* with the MIRO and ZRS, while its strength is apparently enhanced by B_{\parallel} . In addition, employing B_{\parallel} we were also able to uncover a resistively detected resonance which occurs at approximately twice the cyclotron frequency.

Ultraclean 2DES used in these experiments were provided by $\text{Al}_{0.24}\text{Ga}_{0.76}\text{As}/\text{GaAs}/\text{Al}_{0.24}\text{Ga}_{0.76}\text{As}$ square quantum wells (QWs); similar data have been obtained from single-interface $\text{GaAs}/\text{Al}_{0.3}\text{Ga}_{0.7}\text{As}$ heterostructures. Data reported in this paper are from two specimen, sample QW30nm (QW25nm), which is a 30-nm (25-nm) width QW, having an electron density of $n_e = 3.45 \times 10^{11}$ (3.30×10^{11}) cm^{-2} and a mobility of $\mu = 1.8 \times 10^7$ (1.9×10^7) $\text{cm}^2/\text{V s}$ at 0.35 K. These parameters were attained after a brief illumination from a red light-emitting diode at 2 K. Both specimens were lithographically defined and wet-etched: the sample QW30nm is a $200 \mu\text{m} \times 400 \mu\text{m}$ rectangle and the sample QW25nm is a $100 \mu\text{m} \times 2 \text{ mm}$ Hall bar. The measurements were performed in a top-loading He-3 cryostat with a base temperature of 0.35 K; microwaves were generated by Gunn diodes and guided down to the sample via a waveguide, with MW propagating normal to the sample surface. The long-side of the samples was placed in parallel with the wide-side of the waveguide cross section (the direction is denoted by x). Four terminal, low frequency (23 Hz) lock-in technique with an excitation current $I = 1 \mu\text{A}$ was employed. A two-axis Nb superconducting solenoid system was employed to provide a perpendicular field B_z (up to 3 T) and a parallel field B_{\parallel} (up to 2 T).

We have carefully checked against possible contact effects influencing the measured signal in these experiments. In general, any signal from the contact region should have been minimized by the standard four-terminal lock-in technique, this is especially true in lithographically defined

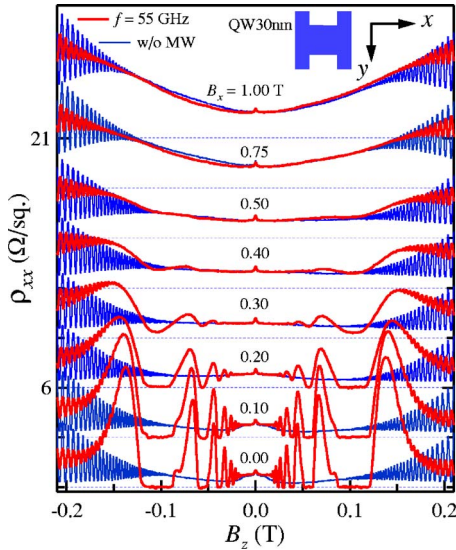


FIG. 1. (Color online) Microwave-induced resistance oscillations and the zero-resistance states observed on a ultrahigh-mobility 2DES (sample QW30nm, see text) subjected to a parallel magnetic field B_x (for clarity, traces are vertically shifted by steps of $3 \Omega/\text{sq.}$). For comparison, corresponding traces without microwave irradiation (thin lines) are also shown.

samples where the contacts are away from the part of 2DES being measured. Since the contacts for the 2DES are exposed to continuous MW irradiation (as were, in fact, in all experimental work previously reported¹⁻⁶), in principle, the photo-voltage, generated near the contacts, can contribute a modulation at the frequency of the excitation current, leading to a measured signal. This modulation originates from the cubic term in the I - V characteristic of a non-ohmic contact. However, as long as the contacts are reasonably ohmic and the MW power is not too large, this rectification effect of contacts are expected to be small. In the photoresistance measurements, our voltage signals were proportional to the low frequency (23 Hz) excitation current (at the order of $1 \mu\text{A}$) and, with zero excitation current, only the noise floor were measured. In addition, the excitation current was essentially unaffected by the MW.¹⁹ Therefore, our measured signals must be a response of 2DES itself, rather than that of the contacts.

An overview of MIRO and ZRS (thick lines) in a parallel magnetic field B_x for sample QW30nm is shown in Fig. 1. The traces were recorded at a temperature $T \approx 1.0 \text{ K}$ while the sample was continuously irradiated by a MW of frequency $f = 55 \text{ GHz}$ and power (at the waveguide section close to the sample surface) $P \approx 100 \mu\text{W}$. For comparison, corresponding magnetoresistivity (MR) without MW (at $T \approx 0.35 \text{ K}$), is also shown (thin lines). At $B_{//} = 0$, the “dark” traces show negative MR around $B_z = 0$ which consist of a hump ($|B_z| \leq 0.025 \text{ T}$) and a sharp peak ($|B_z| \leq 0.003 \text{ T}$) on top of it. In general, with increasing $B_{//}$ this hump disappears rapidly and only the sharp peak close to $B_z = 0$ is left. For all $B_{//}$ applied (up to 2.0 T), sharp Shubnikov-de Haas (SdH) oscillations are observed while their onset moves to higher B_z with increasing $B_{//}$ (from $B_z \sim 0.08 \text{ T}$ at $B_{//} = 0$ to $B_z \sim 0.12 \text{ T}$ at $B_{//} = 1.0 \text{ T}$). With MW irradiation, the most sa-

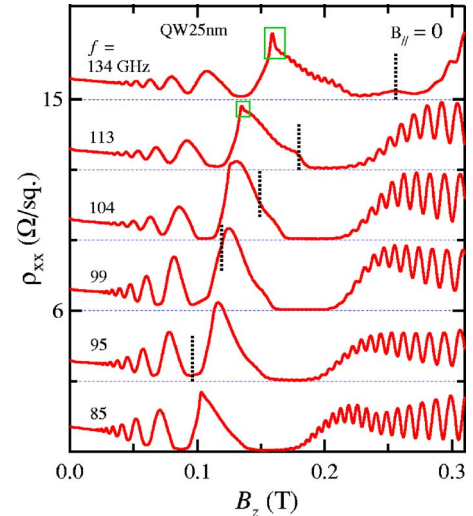


FIG. 2. (Color online) Microwave response of sample QW25nm (described in text) recorded at $B_{//} = 0$ for selected microwave frequencies (traces are vertically shifted by steps of $3 \Omega/\text{sq.}$). The dashed vertical lines indicate the positions of the magnetoplasmon peak, as determined from traces taken at a $B_{//}$ where the magnetoplasmon peak is prominent and easily resolved (see Fig. 3). The $f = 134 \text{ GHz}$ and $f = 113 \text{ GHz}$ traces show an extra peak (framed) on top of the second MIRO maximum, this extra peak generally appears for a wide range of microwave frequencies and is better resolved in $B_{//}$ (see Fig. 3).

lient feature is that the MIRO diminishes rapidly with increasing B_x : at $B_x = 0.2 \text{ T}$, its amplitude has already decreased more than 50% as compared to that at $B_x = 0$; and by $B_x = 0.75 \text{ T}$, it completely disappears. Up to four ZRS are observed at the minima of the MIRO for $B_x = 0$, but all initial ZRS become nonzero at $B_x \geq 0.3 \text{ T}$. As shown in Fig. 1, the strongest first two ZRS (centered around $B_z = 0.10 \text{ T}$ and $B_z = 0.055 \text{ T}$) persist up to $B_x = 0.2 \text{ T}$, but their widths decrease with increasing B_x . We note that, with increasing B_x , the positions of the oscillation maxima shift towards higher B_z while those of the ZRS and oscillation minima remain roughly constant.

By rotating the sample probe 90° , we were able to perform the same measurements with a parallel magnetic field B_y which is perpendicular to the excitation current. The observations are qualitatively the same as those of Fig. 1. However, the effect of B_y on MIRO and ZRS is not as strong as that of B_x : The ZRS disappear at $B \leq 0.5 \text{ T}$ and the MIRO amplitudes reach zero at $B \leq 1.5 \text{ T}$. Despite these quantitative differences, our main finding is that in our two-axis-magnet experiments, the MIRO/ZRS are suppressed by a modest parallel magnetic field $B_{//}$.

In order to study the influence of $B_{//}$ on the resistively-detected MPR, we have performed similar experiments on the Hall bar sample of QW25nm. Not surprisingly, with $B_{//}$ we have also observed a strong suppression of MIRO/ZRS in this sample.²⁰ However, contrary to the case of MIRO/ZRS, the MPR peak is apparently enhanced by $B_{//}$. Typically, the magnetoplasmon peak is masked by the MIRO at $B_{//} = 0$ but becomes dominant at elevated $B_{//}$. As shown in Fig. 2, at $B_{//} = 0$, with low MW frequency the MPR just slightly modi-

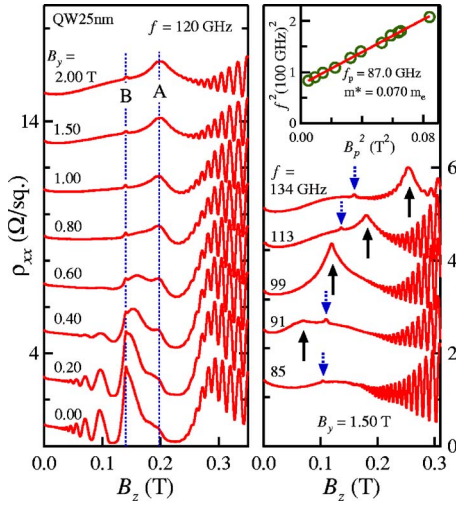


FIG. 3. (Color online) Magnetoplasmon resonance observed on sample QW25nm subjected to a parallel magnetic field. Left panel: Magnetoresistance traces taken at $f=120$ GHz and different B_y 's (vertically shifted with steps of $2 \Omega/\text{sq.}$). In contrast to the diminishing of the MIRO oscillations, the magnetoplasmon resonance (vertical line A) becomes stronger with increasing B_y ; in addition, another weak peak at $\omega/\omega_c \approx 2$ (vertical line B) is also clearly resolved at increased B_y . Right panel: Magnetoresistance traces taken at $B_y=1.50$ T and different MW frequencies (vertically shifted with steps of $1 \Omega/\text{sq.}$). Magnetoplasmon resonance peaks are indicated by up arrows, and the weak peaks at $\omega/\omega_c \approx 2$ are indicated by down arrows. Inset: The plot of f^2 vs B_{\parallel}^2 , which reveals the typical magnetoplasmon dispersion relation.

fies the shape of the MIRO and can only be clearly identified when its position moves up into the wide first minimum of the MIRO, with increasing MW frequency. The enhancement of the MPR peak in an increasing B_{\parallel} , concurrent with the suppression of MIRO, is shown in the left panel of Fig. 3, for $f=120$ GHz as an example. Another important observation is that the peak position of the magnetoplasmon mode is almost independent of B_{\parallel} (within the accuracy of 1%) as indicated by the vertical line A of the left panel of Fig. 3. This means the effective electron mass (m^*) is nearly constant within the B_{\parallel} range studied.

The MPR at various MW frequencies has been explored, example traces recorded at $B_y=1.50$ T for selected MW frequencies are shown in the right panel of Fig. 3. A set of magnetoplasmon peak positions, plotted in the inset of Fig. 3 (right panel), were accurately determined by employing appropriate B_{\parallel} to simultaneously enhance the magnetoplasmon mode and suppress the MIRO. The fit to the dispersion relation Eq. (1) is excellent and it yields $m^*=0.070 m_e$, and a $f_0 \equiv \omega_0/2\pi=87.0$ GHz which is reasonably close to the calculated value of 93 GHz.

In addition, we observed a small sharp peak (marked by the vertical line B in Fig. 3, left panel) which overlaps with the second maximum of the MIRO; the B_z position of this peak does not change with B_{\parallel} and its strength does not have strong dependence on B_{\parallel} . Although the small peak is already discernible for certain frequencies at $B_{\parallel}=0$ (see Fig. 2, for example), it can be recognized as an extra peak only in elevated B_{\parallel} . This new peak has been observed in a wide MW

frequency range (50–150 GHz) and is not correlated with the magnetoplasmon mode (see the right panel of Fig. 3, the small peak appears at $f=85$ GHz where the magnetoplasmon mode is absent). Note this peak is distinct from MIRO by its behavior in B_{\parallel} . Although the nature of this resistance peak is not clear, such a feature may signal a resonance taking place at approximately twice the cyclotron frequency, i.e., $\epsilon \equiv \omega/\omega_c \approx 2$ with $\omega_c = eB_z/m^*$, possibly due to the bolometric effect of the second sub-harmonic of cyclotron resonance.²¹ We have repeated the experiments on a dozen samples of high-mobility 2DES, and found consistent results. We conclude that the suppression of MIRO/ZRS in a B_{\parallel} is a generic feature in our experiments.

The influence of a B_{\parallel} on the MIRO has also been studied in a different experimental setting,²² where the sample was tilted with respect to magnet axis and MW propagation direction. According to Ref. 22, the MIRO/ZRS was still clearly observable under a tilt angle $\theta=80^\circ$, where the region of the first ZRS and the first MIRO peak is within $0.6 < B_{\parallel} < 1.2$ T; the MIRO was found to disappear at $\theta \sim 90^\circ$, but it is attributed by the author to the vanishing of MW flux on the 2DES rather than to the effect of a large B_{\parallel} . Whether MIRO persists between $80^\circ < \theta \leq 90^\circ$, or equivalently at B_{\parallel} beyond 1 T, has not been reported in Ref. 22; it cannot be ruled out at the present that a larger B_{\parallel} would be necessary to suppress the MIRO in their experiments. We should comment that, in these experiments with sample dimensions close to the MW wavelength, “flux” is not a good term to describe the MW strength with respect to the 2DES sample, rather the local MW fields should be directly referred. Even at large tilting angles, the MW field components on the 2DES plane are not negligible,²³ and can be sufficiently large in the high MW power regime relevant to Ref. 22. We therefore believe that an alternative interpretation, i.e., the MIRO is suppressed by a large B_{\parallel} , is plausible for the $\theta \sim 90^\circ$ data of Ref. 22.

At the present, there exists no concrete explanation for the observed strong suppression of MIRO and ZRS by a parallel magnetic field. Our analysis shows that the effect cannot be satisfactorily explained by a simple modification of single-particle energy spectrum and/or scattering parameters of the 2DES in B_{\parallel} .

Possible modification of 2DES energy spectrum by B_{\parallel} can arise due to the finite thickness effect, in which the B_{\parallel} can couple to the orbital motion of the electrons via the vector potential of B_{\parallel} ($=zB_{\parallel}$), resulting in a diamagnetic energy shift ($\Delta E_0 \leq 1$ K at $B_{\parallel}=1.0$ T) and a slightly increased effective mass ($\delta m^*/m^* < 1\%$ at $B_{\parallel}=1.0$ T) in the direction perpendicular to B_{\parallel} .²⁴ Nevertheless, these effects could hardly affect the Landau quantization under a perpendicular magnetic field B_z , because the diamagnetic energy is just a constant shift to the energy origin and the Landau levels is still evenly spaced in spite of the mass anisotropy.²⁴

Scattering processes play an essential role in the current theoretical models proposed to explain the MIRO (see, e.g., Refs. 4, 9, and 10), it is therefore relevant to examine how the B_{\parallel} could affect both the elastic (τ_q) and inelastic scattering times (τ_{in}) in the high-mobility 2DES.

For high mobility 2DES at low temperature, the Landau level broadening, characterized by τ_q , is mainly determined by disorders (impurities and interface roughness). Since the

amount of disorders are fixed, the influence of $B_{//}$ on the Landau level broadening is mediated by the deformation of the subband wave function. For our 2DES (30-nm QW with $n_e \sim 3 \times 10^{11} \text{ cm}^{-2}$) at $B_{//} \sim 1 \text{ T}$, $B_{//}$ -induced intersubband scattering should not be significant, because the cyclotron energy ($\sim 2 \text{ meV}$) is much smaller than the subband splitting ($\geq 15 \text{ meV}$). This point may be supported by our observation, as shown in Fig. 1 by “dark” traces with $B_{//}$ up to 1.0 T, that the resistivity at $B_z=0$ is just increased by 70% and the onset field of SdH is increased by 50%, indicating a scattering-time decreasing less than a factor of 2. We note that modification of scattering times at this scale cannot account for the total suppression of MIRO, since the MIRO has been clearly observed in a sample with a mobility ($\mu \sim 3 \times 10^6 \text{ cm}^2/\text{V s}$)¹ much lower than that of the samples studied in this paper ($\mu \sim 18 \times 10^6 \text{ cm}^2/\text{V s}$).

The inelastic scattering time τ_{in} is difficult to assess experimentally. According to Ref. 10, the MIRO amplitude is proportional to τ_{in} which is determined by the electron-electron interaction at low temperatures. It remains to be understood both theoretically and experimentally how a parallel magnetic field would influence the τ_{in} in the high-mobility 2DES.

The role spin degree of freedom plays in MIRO/ZRS is largely ignored so far in theoretical pictures but should be

examined in the context of our findings. If the spin is only involved via Zeeman interaction, its role is expected to be minimal on the MW response of MIRO/ZRS, because MW-induced inter-Landau-level transitions are spin conserved, due to the separation of spin and spatial coordinates. The situation becomes dramatically different in the presence of spin-orbital interactions: generally the spin states are mixed with the spatial wave functions and spin-flip transitions can then occur between Landau levels. Assuming a significant role of spin-flip transitions on the MIRO/ZRS, the $B_{//}$ can, in principle, affect the MW response through the Zeeman and/or spin-orbit interactions (via its vector potential $zB_{//}$). The validity of this scenario based on spin-flip transitions is interesting to test in experiments.

In summary, in our two-axis magnet experiments we have observed a strong suppression of the microwave-induced resistance oscillations and the subsequent zero-resistance states by a parallel magnetic field. On the contrary, magnetoplasmon resonance peaks, observed concurrently with MIRO/ZRS, are robust in a parallel magnetic field.

We acknowledge helpful discussions with S. Das Sarma, A. H. MacDonald, A. D. Mirlin, F. von Oppen, M. E. Raikh, and M. G. Vavilov. C.L.Y. and R.R.D. were supported by Grant No. NSF DMR-0408671.

-
- ¹M. A. Zudov, R. R. Du, J. A. Simmons, and J. L. Reno, *Phys. Rev. B* **64**, 201311(R) (2001).
- ²R. G. Mani, J. H. Smet, K. von Klitzing, V. Narayanamurti, W. B. Johnson, and V. Umansky, *Nature (London)* **420**, 646 (2002).
- ³M. A. Zudov, R. R. Du, L. N. Pfeiffer, and K. W. West, *Phys. Rev. Lett.* **90**, 046807 (2003); C. L. Yang, M. A. Zudov, T. A. Knuttila, R. R. Du, L. N. Pfeiffer, and K. W. West, *ibid.* **91**, 096803 (2003).
- ⁴S. I. Dorozhkin, *JETP Lett.* **77**, 577 (2003).
- ⁵R. L. Willett, L. N. Pfeiffer, and K. W. West, *Phys. Rev. Lett.* **93**, 026804 (2004).
- ⁶S. A. Studenikin, M. Potemski, P. T. Coleridge, A. S. Sachrajda, and Z. R. Wasilewski, *Solid State Commun.* **129**, 341 (2004).
- ⁷R. R. Du, M. A. Zudov, C. L. Yang, L. N. Pfeiffer, and K. W. West, *Physica E (Amsterdam)* **22**, 7 (2004); M. G. Vavilov and I. L. Aleiner, *Phys. Rev. B* **69**, 035303 (2004), and references therein.
- ⁸A. V. Andreev, I. L. Aleiner, and A. J. Millis, *Phys. Rev. Lett.* **91**, 056803 (2003).
- ⁹A. C. Durst, S. Sachdev, N. Read, and S. M. Girvin, *Phys. Rev. Lett.* **91**, 086803 (2003); J. Shi and X. C. Xie, *ibid.* **91**, 086801 (2003); X. L. Lei and S. Y. Liu, *ibid.* **91**, 226805 (2003).
- ¹⁰I. A. Dmitriev, A. D. Mirlin, and D. G. Polyakov, *Phys. Rev. Lett.* **91**, 226802 (2003); I. A. Dmitriev, M. G. Vavilov, I. L. Aleiner, A. D. Mirlin, and D. G. Polyakov, *Phys. Rev. B* **71**, 115316 (2005).
- ¹¹J. C. Phillips, *Solid State Commun.* **127**, 233 (2003).
- ¹²J. Inarrea and G. Platero, *Phys. Rev. Lett.* **94**, 016806 (2005); *Phys. Rev. B* **72**, 193414 (2005).
- ¹³D. H. Lee and J. M. Leinaas, *Phys. Rev. B* **69**, 115336 (2004).
- ¹⁴S. A. Mikhailov, *Phys. Rev. B* **70**, 165311 (2004); S. A. Mikhailov and N. A. Savostianova, *ibid.* **71**, 035320 (2005).
- ¹⁵I. V. Kukushkin, J. H. Smet, S. A. Mikhailov, D. V. Kulakovskii, K. von Klitzing, and W. Wegscheider, *Phys. Rev. Lett.* **90**, 156801 (2003); I. V. Kukushkin, M. Y. Akimov, J. H. Smet, S. A. Mikhailov, K. von Klitzing, I. L. Aleiner, and V. I. Falko, *ibid.* **92**, 236803 (2004).
- ¹⁶S. A. Studenikin, M. Potemski, A. Sachrajda, M. Hilke, L. N. Pfeiffer, and K. W. West, *Phys. Rev. B* **71**, 245313 (2005).
- ¹⁷For a review, see D. Heitmann, *Surf. Sci.* **170**, 332 (1986).
- ¹⁸E. Vasiliadou, G. Muller, D. Heitmann, D. Weiss, K. v. Klitzing, H. Nickel, W. Schlapp, and R. Losch, *Phys. Rev. B* **48**, 17145 (1993).
- ¹⁹A negligible change ($< 0.1\%$) of the low-frequency excitation current was introduced by the MW, which corresponded to the MW-induced resistance change of the 2DES, as a result of slight modification of the load resistance in the constant-current circuit.
- ²⁰Contrary to sample QW30 nm, the effect of $B_{//}$ on MIRO/ZRS in sample QW25 nm does not show significant anisotropy with respect to the current direction x ; data shown in Fig. 3 are for $B_{//}$ along y direction (B_y).
- ²¹Our data do not manifest the bolometric peak of the primary cyclotron resonance, presumably because it is masked by the SdH oscillations.
- ²²R. G. Mani, *Phys. Rev. B* **72**, 075327 (2005).
- ²³Only for a MW with well-defined polarization direction, the MW electrical field in the 2DES can be zero at tilt angle $\theta=90^\circ$, this also requires the sample-rotating axis perpendicular to the MW polarization direction. As stated in Ref. 22, in their measure-

ments the MW polarization is indeterminate due to the use of an oversized waveguide. Moreover, the MW polarization is also distorted by the presence of metallic contacts and by the reflection of the sample itself. Because of these complications, the

MW electrical field in the 2DES plane is generally nonzero even at tilt angle $\theta=90^\circ$.

²⁴F. Stern and W. E. Howard, Phys. Rev. **163**, 816 (1967); F. Stern, Phys. Rev. Lett. **21**, 1687 (1968).